8-10-2020

Dark sector origin of the KOTO and MiniBooNE anomalies

Alakabha Datta
University of Mississippi

Saeed Kamali
University of Mississippi

Danny Marfatia
University of Hawai'i at Mānoa

Recommended Citation

Datta, A., Kamali, S., & Marfatia, D. (2020). Dark sector origin of the KOTO and MiniBooNE anomalies. Physics Letters B, 807, 135579. https://doi.org/10.1016/j.physletb.2020.135579

Physics Letters B 807 (2020) 135579

Contents lists available at ScienceDirect

Physics Letters B

www.elsevier.com/locate/physletb

Dark sector origin of the KOTO and MiniBooNE anomalies

Alakabha Datta [a], Saeed Kamali [a,*], Danny Marfatia [b]

[a] Department of Physics and Astronomy, University of Mississippi, 108 Lewis Hall, Oxford, MS 38677, USA
[b] Department of Physics and Astronomy, University of Hawaii, Honolulu, HI 96822, USA

ARTICLE INFO

Article history:
Received 21 May 2020
Received in revised form 21 June 2020
Accepted 21 June 2020
Available online 26 June 2020
Editor: J. Hisano

ABSTRACT

We present a dark sector model that reproduces the KOTO, MiniBooNE and muon anomalous magnetic moment anomalies. The dark sector is comprised of a light scalar singlet S that has a large coupling to a slightly heavier sterile neutrino that mixes with the active neutrinos. The scalar couples to standard model fermions via Yukawa couplings, and to photons via a higher-dimensional coupling. The KOTO signal is a result of the flavor-changing penguin process $K_L \to \pi^0 S$ followed by the decay of S to neutrinos. The sterile neutrino produced in neutrino-nucleus scattering at MiniBooNE decays to an active neutrino and S, which decays electromagnetically and creates an event excess at low energies.

1. Introduction

Currently, there are many measurements in the quark and the lepton sectors that have eluded explanation in the standard model (SM). In the quark sector there are several anomalies in the B, D and K systems. Here we concentrate on K decays where the interesting modes are the rare kaon decays, $K_L \to \pi^0 \nu\bar{\nu}$ and $K^+ \to \pi^+ \nu\bar{\nu}$, which are being probed by the KOTO experiment at J-PARC and the NA62 experiment at CERN. Recent reports from KOTO [1,2] indicate that $K_L \to \pi^0 \nu\bar{\nu}$ decays occur at a rate much larger than predicted by the SM [3]. A fair amount of interest has been generated in model building to explain the KOTO anomaly [3–15]. Based on the number of events observed by the KOTO experiment, the branching ratio can be estimated to be [3]

$$BR(K_L \to \pi^0 \nu\bar{\nu})_{\rm KOTO} = 2.1^{+2.0(+4.1)}_{-1.1(-1.7)} \times 10^{-9}\,. \tag{1}$$

This result is two orders of magnitude larger than the SM prediction, $BR(K_L \to \pi^0 \nu\bar{\nu})_{\rm SM} = (3.4 \pm 0.6) \times 10^{-11}$ [16].

On the other hand NA62 obtains a 90% C.L. bound for $K^+ \to \pi^+ \nu\bar{\nu}$ [17],

$$BR(K^+ \to \pi^+ \nu\bar{\nu})_{\rm NA62} < 1.85 \times 10^{-10}\,, \tag{2}$$

which appears to violate the Grossman-Nir (GN) bound [18]

$$BR(K_L \to \pi^0 \nu\bar{\nu}) \leq 4.3 BR(K^+ \to \pi^+ \nu\bar{\nu})\,. \tag{3}$$

The E787 and E949 experiments at BNL have also measured $BR(K^+ \to \pi^+ \nu\bar{\nu})$ [19,20] assuming the pion spectrum predicted by the SM. According to Ref. [20],

$$BR(K^+ \to \pi^+ \nu\bar{\nu}) = (1.73^{+1.15}_{-1.05}) \times 10^{-10}\,, \tag{4}$$

which is also in conflict with the GN bound.

Many solutions to the KOTO anomaly involve a new light particle X that appears in the decay $K \to \pi X$, with X decaying outside the detector. As the KOTO and NA62 detectors have different lengths, by an appropriate choice of parameters, consistency is achievable. Another option is that if the X mass is around the pion mass then there is a range of m_X not probed by NA62 due to the large pion backgrounds from $K^+ \to \pi^0 \pi^+$ [21]; see Fig. 2 of Ref. [4]. This gap in sensitivity occurs for $m_X \sim 100 - 165$ MeV, although if m_X is very close to the pion mass then part of this gap is covered by a different NA62 analysis, which sets a limit on the invisible decays of the neutral pions from $K^+ \to \pi^+ \pi^0$: $BR[\pi^0 \to \text{invisible}] < 4.4 \times 10^{-9}$ [17], which implies $BR[K^+ \to \pi^+ \text{invisible}] \sim 10^{-9}$ [8]. Part of this gap is also covered by E949 [20] which constrains the branching ratio for $K^+ \to \pi^+ X$ as a function of the mass and lifetime of X.

The dark sector model we present in this work has a light scalar, S, in the above mass window to avoid the NA62 constraint. Because a kinetically-mixed Z' cannot explain the KOTO anomaly [7], a scalar mediator is an obvious choice. The scalar interacts with SM particles with coupling strengths proportional to their masses. Our dark sector also includes a sterile neutrino, ν_D, that couples to the scalar with an $\mathcal{O}(1)$ coupling. The coupling of the scalar to active neutrinos is generated by the mixing of the sterile neutrino with the active neutrinos. The model generates

* Corresponding author.
E-mail addresses: datta@phy.olemiss.edu (A. Datta), skamali@go.olemiss.edu (S. Kamali), dmarf8@hawaii.edu (D. Marfatia).

https://doi.org/10.1016/j.physletb.2020.135579

the FCNC transitions, $b \to sS$ and $s \to dS$, through the usual penguin diagrams. The corresponding mesonic level process $K_L \to \pi^0 S$ followed by the decay of S to neutrino pairs explains the KOTO measurement.

The goal of the MiniBooNE experiment was to address the 3.3σ LSND anomaly in electron-like events seen in the $\bar{\nu}_e$ channel [22]. Over the 15 years of data taken by MiniBooNE, a new anomaly, that is not inconsistent with the LSND anomaly, has gained significance. The data show a 4.8σ excess in the low energy part of electron spectra in both the neutrino and antineutrino channels [23]. This *low-energy excess* begs explanation independently of the LSND anomaly.[1] Models in which a light neutrino is upscattered into a sterile neutrino which subsequently decays into an e^+e^- pair have been considered in Refs. [25,26] to resolve this anomaly. The mediator through which the light neutrino scatters on the target nucleus is a Z' boson kinetically mixed with the electromagnetic field tensor. However, the solution in which the Z' is lighter than the sterile neutrino [25] is excluded [27] by data from the CHARM-II [28] and MINERvA [29] experiments. A novel aspect of our model is that electromagnetic decays of the sterile neutrino produced through neutrino-nucleus scattering via S exchange explains the MiniBooNE anomaly and is compatible with CHARM-II and MINERvA data even with S lighter than the sterile neutrino.

There is also the long standing anomaly in the anomalous magnetic moment of the muon, $(g-2)_\mu$. The SM prediction [30] is 3.7σ smaller than the experimental measurement [31]:

$$(g-2)_\mu^{\rm exp} - (g-2)_\mu^{\rm SM} = 27.4\,(2.7)\,(2.6)\,(6.3) \times 10^{-10}\,. \tag{5}$$

The first two uncertainties are theoretical and the last, and largest, is experimental. The experimental uncertainty is expected to be reduced by a factor of four by the Muon $g-2$ Experiment [32] at Fermilab, which is currently collecting data. With the further addition of a higher dimensional coupling to two photons motivated by recent model building [33], the $(g-2)_\mu$ anomaly can also be addressed in our model. A welcome consequence of this coupling is that the scalar dominantly decays to a photon pair which can be misidentified as electron events and reproduces the MiniBooNE anomaly.

The paper is organized as follows. In Section 2, we describe our model and the decays of the scalar and sterile neutrino. In Section 3, we explain the KOTO and the $(g-2)_\mu$ anomalies and demonstrate consistency with all relevant constraints. In Section 4 we consider the production of the sterile neutrino in neutrino scattering experiments, and explain the MiniBooNE anomaly. We summarize in Section 5.

2. Model

The dark sector has a light singlet scalar S, with mass in the range $m_S \sim 100 - 165$ MeV, coupled to a sterile neutrino ν_D which is heavier than the scalar. The scalar has couplings to SM fermions proportional to their masses:

$$\mathcal{L}_S \supset \frac{1}{2}(\partial_\mu S)^2 - \frac{1}{2}m_S^2 S^2 - \eta_d \sum_{f=d,l} \frac{m_f}{v}\bar{f} f S - \eta_u \sum_{f=u} \frac{m_f}{v}\bar{f} f S - g_D S \bar{\nu}_D \nu_D\,. \tag{6}$$

Here $v \simeq 246$ GeV, is the vacuum expectation value of the Higgs boson, d and l correspond to down-type quarks and leptons and u corresponds to up-type quarks. This coupling structure can arise in ultraviolet complete models in which a light scalar singlet is added to a two-Higgs-doublet model [8,33,34]. In this case, the parameters η_d and η_u play the role of the mixing parameters between the singlet scalar and the two neutral scalars of the two-Higgs-doublet model.

The mixing between the flavor eigenstates ν_α and mass eigenstates ν_i of the four Dirac neutrinos is given by

$$\nu_{\alpha(L,R)} = \sum_{i=1}^{4} U_{\alpha i}^{(L,R)} \nu_{i(L,R)}\,, \quad (\alpha = e, \mu, \tau, D)\,, \tag{7}$$

where L, R denote the handedness of the neutrino, and U^L and U^R are 4×4 unitary matrices, which we take to be real and equal ($U^L = U^R \equiv U$). Neutrino mixing induces a coupling of the scalar to light neutrinos. ν_4 must be a Dirac neutrino so that its non-relativistic decays, $\nu_4 \to \nu + S$, are not isotropic [35]. If ν_4 were Majorana, its decays would be approximately isotropic which is inconsistent with the angular distribution measured by MiniBooNE.

To address the $(g-2)_\mu$ anomaly we include the higher-dimensional Lagrangian term,

$$\Delta\mathcal{L}_S = -\frac{1}{4}\kappa S F_{\mu\nu}F^{\mu\nu}\,, \tag{8}$$

which yields an $S\gamma\gamma$ coupling governed by the parameter κ, which has dimensions of inverse mass. This coupling is generically induced by heavy states, such as leptoquarks, and for $\kappa \sim (1\,\text{TeV})^{-1}$, the light scalar can explain the $(g-2)_\mu$ anomaly [33]. In general, a higher dimensional coupling to gluon fields is permitted, which would allow S to decay to hadrons. However, we take $m_S < 2m_\mu$ so that S can only decay to electrons, neutrinos and photons.

The scalar S contributes to $(g-2)_\mu$ via the one-loop and Barr-Zee diagrams [36] in Fig. 1. The Barr-Zee contribution is induced by the effective $S\gamma\gamma$ coupling which is proportional to κ. The one-loop contribution is given by [37],

$$\delta(g-2)_\mu^{(1\text{-loop})} = \frac{\eta_d^2}{8\pi^2}\frac{m_\mu^2}{v^2}\int_0^1 dz \frac{(1+z)(1-z)^2}{(1-z)^2 + r^{-2}z}\,, \tag{9}$$

where $r = m_\mu/m_S$. The Barr-Zee contribution is dominated by the log-enhanced term [38],

$$\delta(g-2)_\mu^{S\gamma\gamma} \approx \frac{\eta_d}{4\pi^2}\frac{\kappa m_\mu^2}{v}\ln\frac{\Lambda}{m_S}\,, \tag{10}$$

where Λ is the cutoff scale which we may take to be of the order of the mass of the particles that induce the effective $S\gamma\gamma$ coupling. We set $\Lambda = 2$ TeV. We will see later that the contribution to $(g-2)_\mu$ is dominated by the $S\gamma\gamma$ coupling.

The decay width of S to all three light neutrinos ($\nu_i,\ i = 1,2,3$) is

$$\Gamma_{S\to\nu\nu} = \frac{g_D^2}{8\pi}(1 - |U_{D4}|^2)^2 m_S\,, \tag{11}$$

and its decay width to e^+e^- is given by

$$\Gamma_{S\to e^+e^-} = \frac{\eta_d^2}{8\pi}\frac{m_e^2 m_S}{v^2}\left(1 - 4\frac{m_e^2}{m_S^2}\right)^{3/2}\,. \tag{12}$$

An expression for its width to photons can be found in Ref. [33].

The decay width of ν_4 to $S\nu$ (with ν denoting all three light neutrinos) is

[1] Accounts of the LSND and MiniBooNE anomalies in terms of oscillations between active neutrinos and an eV-mass sterile neutrino must contend with a raft of experimental constraints, which lead to baroque scenarios as in Ref. [24].

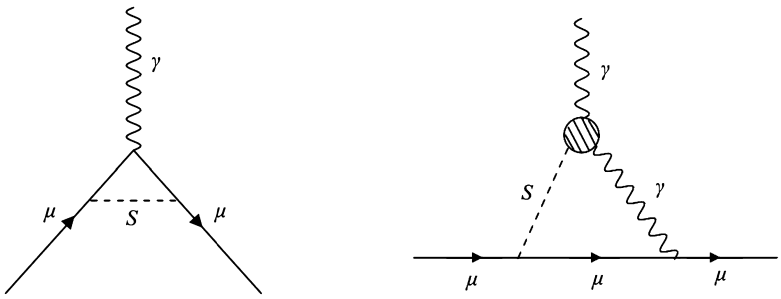

Fig. 1. The scalar S contributions to $(g-2)_\mu$.

$$\Gamma_{\nu_4\to S\nu} = \frac{g_D^2}{8\pi}|U_{D4}|^2\left(1-|U_{D4}|^2\right)\left(1-\frac{m_S^2}{m_{\nu_4}^2}\right)^2 m_{\nu_4}\,. \tag{13}$$

Assuming $U_{e4}\approx U_{\tau 4}\approx 0$, by unitarity we have $1-|U_{D4}|^2=|U_{\mu 4}|^2$. Note that the scalar has a much longer lifetime $\sim|U_{\mu 4}|^{-4}$ than the sterile neutrino $\sim|U_{\mu 4}|^{-2}$.

3. KOTO and $(g-2)_\mu$ anomalies

The coupling of S to up-type quarks leads to the flavor changing neutral transitions $b\to s$ and $s\to d$ via the penguin loop, thus contributing to several rare hadronic decays. We examine two cases:

1. $\kappa\neq 0$: We consider the full Lagrangian and find the parameter values that can explain the KOTO, MiniBooNE and $(g-2)_\mu$ anomalies.
2. $\kappa=0$: We neglect the effective $S\gamma\gamma$ coupling and find the parameters that can explain the KOTO and MiniBooNE anomalies, but not the $(g-2)_\mu$ anomaly.

In the B and K systems, the off-shell effects of the scalar mediator are sub-dominant and place only weak constraints on the parameters of the model. The full list of such constraints is provided in Ref. [33]. The main constraints therefore come from on-shell production of the scalar S. (Obviously, when the $S\gamma\gamma$ coupling is neglected, the constraints with $\gamma\gamma$ final states are not taken into account.) The primary constraints are

- $K_L\to\pi^0 e^+e^-$: We require $BR(K_L\to\pi^0e^+e^-)<2.8\times10^{-10}$ [39].
- $K_{L,S}\to\pi^0\gamma\gamma$: For these decay modes, we take the scalar contribution to be smaller than their measured central values: $BR(K_L\to\pi^0\gamma\gamma)=(1.273\pm0.033)\times10^{-6}$ and $BR(K_S\to\pi^0\gamma\gamma)=(4.9\pm1.8)\times10^{-8}$ [40].
- $K^+\to\pi^+\gamma\gamma$: We require the branching ratio to be smaller than the central value of the measurement, $BR(K^+\to\pi^+\gamma\gamma)=(1.01\pm0.06)\times10^{-6}$ [40]. Note that this is a non-resonant measurement that corresponds to diphoton invariant masses above the range of S masses we consider here.
- $K^+\to\pi^+\nu\bar\nu$: We require $BR(K^+\to\pi^+\nu\bar\nu)<10^{-9}$, obtained by NA62 if the scalar mass is close to the pion mass [17].
- $B\to K^{(*)}\gamma\gamma$: This decay mode has not been measured. We require the scalar contribution to satisfy $BR(B\to K^{(*)}\gamma\gamma)<10^{-4}$ because for a fraction of the events the two photons could be misidentified as a single photon leading to a signal in $B\to X_s\gamma$ [40].
- $B\to K^*e^+e^-$: This decay is measured at LHCb [41]. We require the branching ratio to lie within 1σ of the measured value, $BR(B\to K^*e^+e^-)=(3.1^{+0.9+0.2}_{-0.8-0.3}\pm0.2\pm0.5)\times10^{-7}$; the last uncertainty is the theoretical uncertainty.

With the full Lagrangian, we resolve the $(g-2)_\mu$ anomaly within 1σ and the KOTO anomaly at 95% C.L. In Table 1 we provide benchmark points that solve the KOTO, MiniBooNE and $(g-2)_\mu$ anomalies and satisfy the above constraints. Their corresponding branching fractions to various modes are as in Table 2. Note that the 90% C.L. experimental constraint, $B\to K^{(*)}\nu\bar\nu<2.6(1.8)\times10^{-5}$ [40], is easily satisfied by the benchmark points. The interesting signals of the model are $B\to K^{(*)}\gamma\gamma$ and $K\to\pi\gamma\gamma$ decays via resonant production of S, with branching ratios, $\sim10^{-5}$ and 10^{-7}, respectively.

4. MiniBooNE anomaly

The sterile neutrino is produced via coherent or incoherent scattering of an active neutrino on a nucleus through scalar exchange, $\nu_\mu+N\to\nu_4+N$. The effective coupling generated by the interaction term in Eq. (6) and neutrino mixing is $g_D U_{\mu4}|U_{D4}|^2 S\,\bar\nu_{4R}\nu_{\mu L}$. To calculate the coherent scattering cross section mediated by the scalar S, we define the coupling between the nucleus and the scalar C_N:

$$\mathcal{L}_{SN}=C_N S\bar\psi_N\psi_N\,, \tag{14}$$

where ψ_N is the spinor of the nucleus and C_N is related to the couplings of the scalar to the proton (C_p) and neutron (C_n),

$$C_N=ZC_p+(A-Z)C_n\,, \tag{15}$$

where Z and $A-Z$ are the numbers of protons and neutrons in the nucleus, respectively. The nucleon couplings are in turn related to the quark-scalar couplings, $\eta_u\frac{m_u}{v}$ for up-type quarks and $\eta_d\frac{m_d}{v}$ for down-type quarks:

$$C_p=\frac{m_p}{v}\left(\sum_u\eta_u f_u^p+\sum_d\eta_d f_d^p\right),$$
$$C_n=\frac{m_n}{v}\left(\sum_u\eta_u f_u^n+\sum_d\eta_d f_d^n\right). \tag{16}$$

Here m_p and m_n are the proton and neutron masses, and f^p and f^n are the proton and neutron form factors [42–44]. Note that for our choice of quark couplings, the nucleon couplings of the scalar are independent of the quark masses.

The coherent scattering cross section is

$$\frac{d\sigma_S}{dT}=\frac{g_D^2}{16\pi}|U_{\mu4}C_N|^2|U_{D4}|^4\frac{(2M+T)(m_{\nu_4}^2+2MT)}{E_{\nu_\mu}^2(m_S^2+2MT)^2}F^2(T)\,, \tag{17}$$

where T is the recoil energy, E_{ν_μ} is the muon neutrino energy, M is the mass of the nucleus, and $F(T)$ is the nuclear form factor [45]. For our benchmark points, coherent scattering dominates incoherent scattering at CHARM-II overwhelmingly, and by about

Table 1
Benchmark points with $\kappa \neq 0$ solve the KOTO, MiniBooNE and $(g-2)_\mu$ anomalies and satisfy constraints from kaon decays, B decays, and neutrino scattering data from CHARM-II. For $\kappa = 0$, the $(g-2)_\mu$ anomaly is unsolved.

Benchmark point	κ (TeV^{-1})	$\eta_u \times 10^2$	η_d	g_D	$U_{\mu 4} \times 10^3$	m_S (MeV)	m_{ν_4} (MeV)
1	0.42	0.20	0.56	0.29	4.5	133	416
2	0.87	0.75	0.27	1.9	1.2	113	417
3	1.4	0.22	0.15	1.2	3.9	116	443
4	0.61	0.31	0.39	0.59	3.0	109	462
5	0	0.065	0.89	3.0	2.6	134	402
6	0	0.070	0.87	3.2	2.5	129	408

Table 2
Observables for the benchmark points in Table 1.

Benchmark point	$BR(S \to \gamma\gamma)$	$BR(S \to e^+e^-) \times 10^3$	$BR(S \to \nu\bar{\nu}) \times 10^2$	$BR(B \to K^{(*)}S) \times 10^5$	$BR(K^+ \to \pi^+ S) \times 10^7$	$BR(K_L \to \pi^0 S) \times 10^7$
1	0.911	3.2	8.5	0.19	0.063	0.27
2	0.994	0.26	0.54	2.7	0.92	4.0
3	0.901	0.026	9.9	0.23	0.076	0.32
4	0.946	1.2	5.2	0.45	0.15	0.65
	$BR(S \to \gamma\gamma) \times 10^4$	$BR(S \to e^+e^-) \times 10^3$	$BR(S \to \nu\bar{\nu})$	$BR(B \to K^{(*)}S) \times 10^7$	$BR(K^+ \to \pi^+ S) \times 10^{10}$	$BR(K_L \to \pi^0 S) \times 10^9$
5	5.5	8.8	0.991	2.0	6.7	2.9
6	4.3	7.5	0.992	2.4	7.9	3.4

25%-50% at MiniBooNE. We therefore include an incoherent contribution only for MiniBooNE.

Rather than analyzing MiniBooNE and CHARM-II data, we apply the results of Refs. [25] and [27], which were obtained in the context of a dark Z' mediator kinetically mixed with the electromagnetic field, to our scalar mediator, with suitable modifications. To ensure that our model explains the MiniBooNE anomaly we impose the following constraints:

(i) We require $\int \Phi \frac{d\sigma_S}{dT} dT dE_{\nu_\mu} \times (BR[S \to e^+e^-] + BR[S \to \gamma\gamma])$ to be within 5% of the value of $\int \Phi \frac{d\sigma_{Z'}}{dT} dT dE_{\nu_\mu} \times BR[Z' \to e^+e^-]$ found for the Z' benchmark point in Ref. [25] to explain the MiniBooNE anomaly. Here, Φ is the ν_μ flux at the Booster Neutrino Beam in the neutrino run [46], and σ_S and $\sigma_{Z'}$ are scattering cross sections, including coherent and incoherent contributions, for the scalar and Z' mediators, respectively.

(ii) We implement the CHARM-II constraint in Ref. [27] (which excludes the Z' model of Ref. [25]) by requiring $\sigma_S \times (BR[S \to e^+e^-] + BR[S \to \gamma\gamma]) < \sigma_{Z'} \times BR[Z' \to e^+e^-]$ at CHARM-II for $\langle E_{\nu_\mu} \rangle = 20$ GeV [40], where the right-hand-side is evaluated for the parameter values in Fig. 3 of Ref. [27] with $|U_{\mu 4}| = 10^{-4}$.

(iii) We require $m_{\nu 4} > 400$ MeV so that less than 70% of the excess events are in the most forward bin ($0.8 < \cos\theta < 1$) of the angular distribution of electron-like events at MiniBooNE [27].

The benchmark points in Table 1 satisfy these constraints. For $\kappa = 0$, solutions occur only in narrow parameter ranges. A nonzero κ opens up the parameter space by facilitating a substantial branching fraction to $\gamma\gamma$ which mimics the MiniBooNE signal. Both the scalar and the sterile neutrino are short lived and have rest-frame decay lengths shorter than 0.1 mm, thereby evading bounds from experiments that probe long lived particles. While we conclude that our benchmark points resolve the KOTO, MiniBooNE and $(g-2)_\mu$ anomalies, for a full verification a detailed simulation is necessary which is beyond the scope of this work. Solutions that explain the MiniBooNE anomaly and that are compatible with CHARM-II data arise because our mediator is a scalar particle. For the light (vector) Z' mediator, the scattering cross section gets enhanced which is in conflict with CHARM-II data for the couplings and mixing needed to explain MiniBooNE data. The difference in cross sections arises from the longitudinal polarization of the Z' propagator $\sim q^\mu q^\nu / m_{Z'}^2$, where q is the momentum transfer in the scattering process. For the CHARM-II experiment, $M \simeq \langle E_{\nu_\mu} \rangle \simeq 20$ GeV, so that $\sigma_{Z'}/\sigma_S \sim (M/m_{Z'})^2$ for $m_S \lesssim m_{\nu_4} \ll M$.

5. Summary

We presented a model with a $100 - 140$ MeV singlet scalar S and a $400 - 465$ MeV sterile neutrino ν_D that resolves the KOTO, MiniBooNE and $(g-2)_\mu$ anomalies. S couples to ν_D with an $\mathcal{O}(1)$ coupling and to standard model fermions with Yukawa couplings. A higher-dimensional $S\gamma\gamma$ is needed to address the discrepancy in $(g-2)_\mu$. The scalar couples to active neutrinos through the mixing of the sterile neutrino with active neutrinos. The model generates the FCNC transitions, $b \to s$ and $s \to d$, via penguin diagrams. The resulting $K_L \to \pi^0 S$ transition followed by the decay of S to neutrinos explains the KOTO signal. At MiniBooNE, the sterile neutrino is produced in neutrino-nucleus scattering mediated by the scalar exchange. The subsequent decay of the sterile neutrino to an active neutrino and S, which in turn decays to e^+e^- or $\gamma\gamma$, creates the low-energy excess in the electron-like event data at MiniBooNE. The scenario is compatible with CHARM-II data. Predictions of the model include $B \to K^{(*)}\gamma\gamma$ and $K \to \pi\gamma\gamma$ decays via resonant production of S, with branching ratios, $\sim 10^{-5}$ and 10^{-7}, respectively.

Declaration of competing interest

The authors declare that they have no known competing financial interests or personal relationships that could have appeared to influence the work reported in this paper.

Acknowledgements

We thank Jonathan Feng, Jacky Kumar and Carlos Wagner for useful discussions. This work was financially supported in part by NSF Grant No. PHY-1915142 (A.D.), and DOE Grant No. desc0010504 (D.M.).

References

[1] M.A. Hutcheson, KOTO, in: Meeting of the Division of Particles and Fields of the American Physical Society (DPF2019), Boston, Massachusetts, July 29–August 2, 2019, 2019, arXiv:1910.07585.
[2] B. Beckford, KOTO, arXiv:1910.07148, 2019.
[3] T. Kitahara, T. Okui, G. Perez, Y. Soreq, K. Tobioka, Phys. Rev. Lett. 124 (2020) 071801, arXiv:1909.11111.
[4] D. Egana-Ugrinovic, S. Homiller, P. Meade, arXiv:1911.10203, 2019.

[5] P.S.B. Dev, R.N. Mohapatra, Y. Zhang, arXiv:1911.12334, 2019.
[6] T. Li, X.-D. Ma, M.A. Schmidt, arXiv:1912.10433, 2019.
[7] Y. Jho, S.M. Lee, S.C. Park, Y. Park, P.-Y. Tseng, J. High Energy Phys. 04 (2020) 086, arXiv:2001.06572.
[8] J. Liu, N. McGinnis, C.E.M. Wagner, X.-P. Wang, arXiv:2001.06522, 2020.
[9] J.M. Cline, M. Puel, T. Toma, J. High Energy Phys. 05 (2020) 039, arXiv:2001.11505.
[10] X.-G. He, X.-D. Ma, J. Tandean, G. Valencia, arXiv:2002.05467, 2020.
[11] R. Ziegler, J. Zupan, R. Zwicky, arXiv:2005.00451, 2020.
[12] Y. Liao, H.-L. Wang, C.-Y. Yao, J. Zhang, arXiv:2005.00753, 2020.
[13] X.-G. He, X.-D. Ma, J. Tandean, G. Valencia, arXiv:2005.02942, 2020.
[14] S. Gori, G. Perez, K. Tobioka, arXiv:2005.05170, 2020.
[15] M. Hostert, K. Kaneta, M. Pospelov, arXiv:2005.07102, 2020.
[16] A.J. Buras, D. Buttazzo, J. Girrbach-Noe, R. Knegjens, J. High Energy Phys. 11 (2015) 033, arXiv:1503.02693.
[17] G. Ruggiero, New results on $K^+ \to \pi^+ \nu\bar{\nu}$ from the NA62 experiment, https://indico.cern.ch/event/769729/contributions/3510938/attachments/1905346/3146619/kaon2019_ruggiero_final.pdf, 2019.
[18] Y. Grossman, Y. Nir, Phys. Lett. B 398 (1997) 163, arXiv:hep-ph/9701313.
[19] S. Adler, et al., Phys. Rev. D 77 (2008) 052003.
[20] A.V. Artamonov, et al., BNL-E949, Phys. Rev. D 79 (2009) 092004, arXiv:0903.0030.
[21] K. Fuyuto, W.-S. Hou, M. Kohda, Phys. Rev. Lett. 114 (2015) 171802, arXiv:1412.4397.
[22] A. Aguilar-Arevalo, et al., LSND, Phys. Rev. D 64 (2001) 112007, arXiv:hep-ex/0104049.
[23] A. Aguilar-Arevalo, et al., MiniBooNE, Phys. Rev. Lett. 121 (2018) 221801, arXiv:1805.12028.
[24] J. Liao, D. Marfatia, K. Whisnant, Phys. Rev. D 99 (2019) 015016, arXiv:1810.01000.
[25] E. Bertuzzo, S. Jana, P.A. Machado, R. Zukanovich Funchal, Phys. Rev. Lett. 121 (2018) 241801, arXiv:1807.09877.
[26] P. Ballett, S. Pascoli, M. Ross-Lonergan, Phys. Rev. D 99 (2019) 071701, arXiv:1808.02915.
[27] C.A. Argüelles, M. Hostert, Y.-D. Tsai, Phys. Rev. Lett. 123 (2019) 261801, arXiv:1812.08768.
[28] P. Vilain, et al., CHARM-II, Phys. Lett. B 335 (1994) 246.
[29] E. Valencia, et al., MINERvA, Phys. Rev. D 100 (2019) 092001, arXiv:1906.00111.
[30] T. Blum, P.A. Boyle, V. Gülpers, T. Izubuchi, L. Jin, C. Jung, A. Jüttner, C. Lehner, A. Portelli, J.T. Tsang, RBC UKQCD, Phys. Rev. Lett. 121 (2018) 022003, arXiv:1801.07224.
[31] G.W. Bennett, et al., Muon g-2, Phys. Rev. D 73 (2006) 072003, arXiv:hep-ex/0602035.
[32] J. Grange, et al., Muon g-2, arXiv:1501.06858, 2015.
[33] A. Datta, J.L. Feng, S. Kamali, J. Kumar, Phys. Rev. D 101 (2020) 035010, arXiv:1908.08625.
[34] B. Batell, N. Lange, D. McKeen, M. Pospelov, A. Ritz, Phys. Rev. D 95 (2017) 075003, arXiv:1606.04943.
[35] A.B. Balantekin, A. de Gouvea, B. Kayser, Phys. Lett. B 789 (2019) 488, arXiv:1808.10518.
[36] S.M. Barr, A. Zee, Phys. Rev. Lett. 65 (1990) 21; Erratum: Phys. Rev. Lett. 65 (1990) 2920.
[37] J.P. Leveille, Nucl. Phys. B 137 (1978) 63.
[38] H. Davoudiasl, W.J. Marciano, Phys. Rev. D 98 (2018) 075011, arXiv:1806.10252.
[39] A. Alavi-Harati, et al., KTeV, Phys. Rev. Lett. 93 (2004) 021805, arXiv:hep-ex/0309072.
[40] M. Tanabashi, et al., Particle Data Group, Phys. Rev. D 98 (2018) 030001.
[41] R. Aaij, et al., LHCb, J. High Energy Phys. 05 (2013) 159, arXiv:1304.3035.
[42] A. Crivellin, M. Hoferichter, M. Procura, Phys. Rev. D 89 (2014) 054021, arXiv:1312.4951.
[43] M. Hoferichter, J. Ruiz de Elvira, B. Kubis, U.-G. Meißner, Phys. Rev. Lett. 115 (2015) 092301, arXiv:1506.04142.
[44] P. Junnarkar, A. Walker-Loud, Phys. Rev. D 87 (2013) 114510, arXiv:1301.1114.
[45] R.H. Helm, Phys. Rev. 104 (1956) 1466.
[46] A. Aguilar-Arevalo, et al., MiniBooNE, Phys. Rev. D 79 (2009) 072002, arXiv:0806.1449.